Biochemistry and Biophysics Reports 20 (2019) 100706

Contents lists available at ScienceDirect

Biochemistry and Biophysics Reports

journal homepage: www.elsevier.com/locate/bbrep

Identification and characterization of *Schizophyllum commune* type I metacaspases

Lakhena Leang, Molly C. McDonald, Charlotte R. Mineo, Brandon Jones, Travis Barker, Connor Gagliardi, Kristin M. Fox*

Department of Chemistry, Union College, Schenectady, NY, 12308, USA

ARTICLE INFO

Keywords:
Fungal metacaspase
Calcium response
Protease substrate
Autoproteolysis

ABSTRACT

The role of programmed cell death in filamentous fungi is not well-understood, but is important due to the role of fungi in opportunistic infections. Plants, fungi and protozoa do not have caspase genes, but instead express the homologous proteins denoted metacaspases. To better understand the role of metacaspases in fungi we present an analysis of the sequences and activities of all five Type I metacaspases from *Schizophyllum commune* (*Sc*MC), a mushroom-forming basiodmycete that undergoes sexual reproduction. The five Type I metacaspases of *S. commune* can be divided into two groups based on sequence similarity. Enzymes both with and without the N-terminal prodomain are active, but here we report on the constructs without the prodomains (Δpro). All five *Sc*MCΔpro proteins show the highest enzymatic activity between pH 7 and 8 and require calcium for optimal activity. Optimal Ca^{2+} concentrations for *Sc*MC1Δpro and *Sc*MC2Δpro are 50 mM, while *Sc*MC3, *Sc*MC4Δpro and *Sc*MC5Δpro activity is optimal around 5 mM calcium. All five *S. commune* metacaspases have similar substrate specificity. They are most active with Arg in the P1 position and inactive with Asp in the P1 position.

1. Introduction

Processes of programmed cell death (PCD) are of interest throughout all kingdoms of life. While long-studied in metazoans [1], the role of PCD in filamentous fungi has only been investigated more recently and is not well understood (reviewed in Ref. [2]). Caspase proteins are key components of PCD pathways in metazoans, and their complex role has been clearly elucidated in many studies [3]. Plants, fungi and protozoa do not have caspase genes, but do express the homologous proteins denoted metacaspases (EC# 3.4.22.-) [1]. Metacaspase sequences and structures are similar to those of caspases and contain equivalent active site residues, but have different cleavage specificities [4]. Unlike caspases which cleave most efficiently after Asp, metacaspases cleave most efficiently after Arg and Lys [5]. In filamentous fungi PCD plays a role in development, reproduction, responses to stress, and plant invasion [2,6]. Recent studies indicate that the proteolytic activity of metacaspases is involved in PCD, but the details of this role are not yet clear [7].

Metacaspases are members of the MEROPS C14 family of proteases based on the geometry of the active site residues [8], and have been divided into types I-III (reviewed in Ref. [9]). All three types contain a strongly conserved p20 catalytic region with a Cys-His catalytic dyad similar to that found in caspases. The three types of metacaspases also have a smaller p10 region with high sequence similarity but unclear function. The p20 and p10 regions are connected by a region of low sequence similarity that varies in length. Only the Type I metacaspases contain a long N-terminal region in the same position as the prodomain in caspases. The genomes of multicellular organisms typically encode multiple Type I and Type II metacaspases, while Type III metacaspases have only been identified in a few organisms [10].

The structures of two type I metacaspases have been determined [11,12], but no structures of Type II or Type III metacaspases are known. Type I metacaspase structures are comprised of a core caspase-hemoglobinase fold with a central 8-stranded β-sheet. In both structures the catalytic Cys is located in the loop between β-strands 4 and 5, analogous to the location of the active site loop in caspase-7 [4]. Unlike in caspases, β-strand 5 is not adjacent to β-strand 4, and the linker loop between these strands is much shorter in metacaspases. These observations are consistent with the fact that Type I metacaspases are active as intact monomers [5,11] rather than requiring the proteolytic processing typical of caspases [13].

Metacaspases from plants, protozoa and fungi preferentially cleave after Arg in most *in vitro* studies on fluorogenic peptide substrates [5] and have

* Corresponding author.
E-mail addresses: lakhenal@gmail.com (L. Leang), mollycmcdonald@gmail.com (M.C. McDonald), mineoc@union.edu (C.R. Mineo), brandonmarshalljones@gmail.com (B. Jones), traviss.barker@gmail.com (T. Barker), connor.gagliardi@gmail.com (C. Gagliardi), foxk@union.edu (K.M. Fox).

https://doi.org/10.1016/j.bbrep.2019.100706
Received 24 December 2018; Received in revised form 1 November 2019; Accepted 4 November 2019
Available online 20 November 2019

significantly lower activity when presented with Lys-containing peptides. In contrast, when examining self-cleavage sites, both Arg and Lys are found at sites internal to metacaspases [5,14]. Some metacaspases require calcium for activity [12,15], although whether calcium directly increases autocatalysis or causes a general increase in activity is unclear. Recent work has suggested a role for the p10 region in calcium binding in the metacaspase from the alga *Guillardia theta* [10]. A physiological role for calcium in non-self recognition, a part of the mating process in filamentous fungi, has been identified [2]. Calcium also broadens substrate sequence recognition in a *T. brucei* metacaspase [14].

To better understand the role of metacaspases in fungi we present an analysis of the sequences and activities of all five Type I metacaspases from *Schizophyllum commune* (abbreviated *Sc*MC), a mushroom-forming basiodmycete that undergoes sexual reproduction.

2. Materials and methods

2.1. Identification and alignment of metacaspases

Metacaspases were initially identified by searching the genome of *S. commune* at the JGI [16] with the sequence of the *Saccharomyces cerevisiae* metacaspase MCA1(Q08601, also known as Yca1) as a query using a similarity cutoff of $E > 10^{-5}$. Sequences were aligned using ClustalOmega [17].

2.2. Cloning

The original cDNA template for cloning of *S. commune* metacaspase (*Sc*MC) genes was generated from *S. commune* strain T26 (Fungal Genetics Stock Center #9300). Compatible PCR products of the small ubiquitin-related modifier (SUMO)-containing vector [modified by removing the LIC region from pET His6 Sumo TEV LIC cloning vector (2S-T), a gift from Scott Gradia (Addgene plasmid # 29711)] and the metacaspase encoding fragments were amplified (SI Tables 1–3). Metacaspase fragments both with and without (Δpro) the N-terminal prodomain were generated. Assembly reactions were prepared following the manufacturer's instructions (New England Biolabs) including a 2:1 ratio of metacaspase-encoding fragment to SUMO vector backbone fragment. After a 15 min incubation at 50 °C, NEB 5alpha chemically competent *E. coli* were transformed with the assembly product. Sequences of purified plasmid DNA were confirmed by Sanger sequencing.

Site-directed mutagenesis was performed on sequence-verified plasmids. The plasmid was PCR amplified using primers (SI Tables 1–3) generated by NEBase changer software (New England Biolabs). After amplification of the mutant plasmids, KLD treatment and transformation were performed according to the manufacturer's instructions. All mutant plasmid sequences were confirmed by Sanger sequencing.

2.3. Expression and purification

Chemically competent BL21(DE3) cells were transformed using heat shock with the SUMO-*Sc*MC plasmids containing a His-Tag N-terminal to SUMO. Transformants were incubated at 37 °C and 250 rpm until OD_{600} = 0.5–0.7 (4–6 h). The starter culture was added to 100–500 mL LB medium and carbenicillin (0.05 mg/mL) and incubated for a minimum of 10 h at 27 °C and 250 rpm. (No protein is expressed if cultures are grown at 37 °C.) Cell pellets were stored at -20 °C or -80 °C.

Cell pellets were resuspended in 1.5 mL 1X CelLytic B (10X from Sigma-Aldrich, diluted with 40 mM Tris, pH 8.0) per gram of cell pellet. Following resuspension, 1.5 μL of 5 mg/mL DNaseI was added per gram of cell pellet. The cell suspension was vortexed for 2 min and incubated at 37 °C for 20 min. The supernatant was stored on ice, and the extraction was repeated using 1 mL of 1X CelLytic B and 20 μL of 5 mg/mL DNase I per gram of cell pellet. The supernatants were combined and loaded onto 200 μL of HIS-Select Nickel Affinity Gel beads (Sigma-Aldrich), previously equilibrated with Wash Buffer (50 mM sodium phosphate, 0.3 M NaCl, pH 8.0), for every 1 ml of supernatant. The beads were incubated with rocking at 4 °C for a minimum of 10 h and then washed twice with Wash Buffer. Protein was eluted by incubation at 4 °C for 10 min in Elution Buffer (250mM imidazole, 50mM sodium phosphate, 0.3 M NaCl, pH = 8.0). Recovered protein was aliquoted and used immediately or stored in Elution Buffer plus 30% v/v glycerol at -20 °C. Protein does not maintain activity if frozen and thawed.

Purification was confirmed via protein gel electrophoresis on 12% Tris-glycine polyacrylamide gels and western blot with a His-Tag mouse antibody (1:3,000 dilution of Cell Signaling Technology 27E8) as the primary antibody, and goat anti-mouse (1:10,000 dilution of Invitrogen 626520) as the secondary antibody.

2.4. Activity assays

Assays were performed at room temperature in microplate wells with a total volume of 200 μL containing MC Assay Buffer (50 mM Tris @ pH 7.5, 100 mM NaCl, 5–75 mM $CaCl_2$), 5 mM DTT, 10 μM substrate [Z-GGR-AMC or other fluorogenic peptide (Bachem)], and metacaspase protein at a concentration that gives a rate between 0.1-1.5 RFU/s. Fluorescence at an excitation of 355 nm and an emission of 460 nm was monitored in a Spectramax M3 microplate reader (Molecular Devices) for 10 min at 25 °C. When optimizing pH from 4-10, the MC Assay buffer contained a mixture of 25 mM glycine, 25 mM acetic acid, 25 mM MES, and 75 mM Tris buffers that was titrated to the appropriate pH, 100 mM NaCl and 5 mM $CaCl_2$ (*Sc*MC3, *Sc*MC4, *Sc*MC5) or 75 mM $CaCl_2$ (*Sc*MC 1 and *Sc*MC2).

3. Results and discussion

3.1. ScMC sequences

The five metacaspase sequences including the prodomain are between 350-473 amino acids in length, a considerable difference (Fig. 1). The size variation narrows to 254–296 amino acids without the prodomains. Although some metacaspases contain zinc finger motifs in the

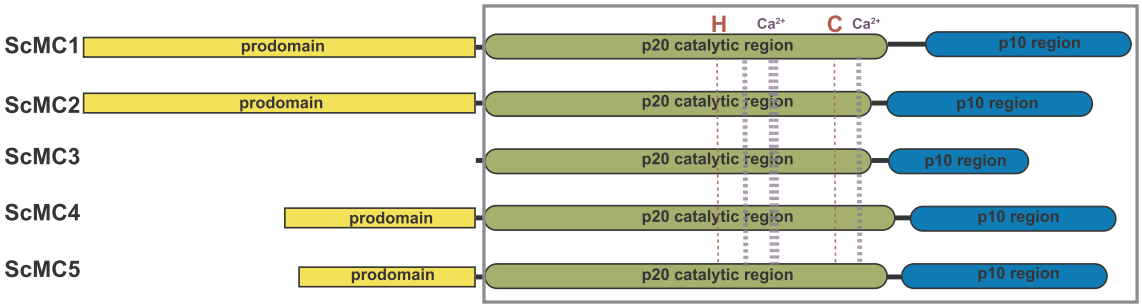

Fig. 1. Visual representation of full-length *Sc*MC1-5 protein domains to scale. The constructs without the prodomain are enclosed by the gray box, and the catalytic Cys and His (red) and the calcium-binding region (purple) are indicated.

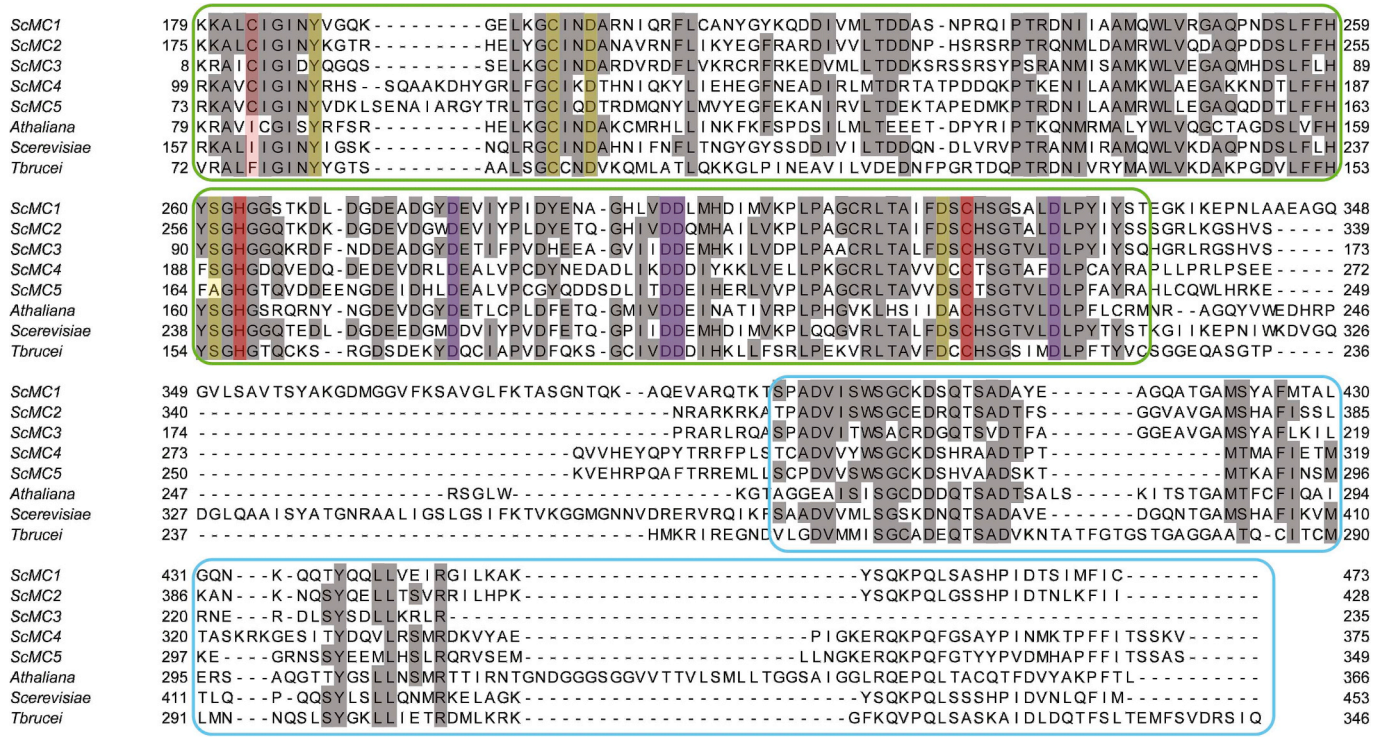

Fig. 2. Sequence alignment of the five Type I metacaspases from *S. commune* and the metacaspases from *S. cerevisiae* (Yca1), *T. brucei* (*Tb*MCA2), and *A. thaliana* (*At*MC1). Conserved residues are shaded in gray. The p20-like and p10-like regions are outlined with green and blue, respectively. Important residues are highlighted: active site (red), the putative calcium binding site (purple), the putative S1 binding site (yellow), and the alternative Cys (light red). Image generated with Jalview.

prodomain, sequence analysis of the *S. commune* metacaspases did not result in the identification of any commonly observed motifs other than the metacaspase C14 protease fold [18].

The five Type I metacaspases of *S. commune* can be divided into two groups based on sequence similarity. *Sc*MC1-3 are 50–62% identical to each other and *Sc*MC4 and 5 are 55% identical, but sequences in one group are only 30–45% identical to members of the other group. Four out of the five *S. commune* metacaspases contain a typical N-terminal prodomain region, with *Sc*MC3 being the only exception. *Sc*MC3 lacks both the prodomain typical of Type I metacaspases and the long linker region typical of Type II metacaspases. As such, it is best described as a Type I metacaspase with a very short prodomain-like region. In addition to the prodomain, each *Sc*MC contains both the p20 and p10 domains characteristic of caspases and metacaspases. The locations of the *Sc*MC prodomain and p20 and p10 region boundaries were identified by sequence alignment with the *A. thaliana* metacaspase 1 (*At*MC1) (Fig. 2).

Overall, the p20 sequence is highly conserved (43–70% identical) among the *Sc*MC sequences, and the p10 is less well conserved, but still significantly similar (32–63% identical) (Fig. 2). The sequence linking the p20 and p10 regions is not conserved and varies in length (Fig. 2). The N-terminal region is poorly conserved among *Sc*MC sequences and also poorly conserved when compared with the sequences of metacaspases in other fungi, plants and *T. brucei* (SI Fig. 2).

In addition to the overall conservation of the p20 and p10 regions, the active site His and Cys are present in all *Sc*MC sequences. The four Asp residues implicated in calcium binding and the residues important for substrate binding in *T. brucei* MCA2 [11] are also highly conserved. A Cys near the beginning of the p20 region is conserved in all five *Sc*MC proteins (Fig. 2), and has been shown to act as an alternative catalytic residue in other metacaspases [9].

In the N-terminal region there are greater similarities between *Sc*MC1 and *Sc*MC2 than between *Sc*MC4 and *Sc*MC5 (SI Fig. 2). An Lsd1-type zinc finger (consensus sequence CXXC) was identified in the N-terminal region of plant metacaspases [5], but is not present in any of the *Sc*MC sequences. In fact, there are no Cys in the regions that are N-terminal to the p20 except for a single residue in *Sc*MC4. In the crystal structure of the *T. brucei* metacaspase (*Tb*MCA2), Tyr 31 is located in the active site in the crystal structure and is proposed to be responsible for preventing autoprocessing in that metacaspase [11]. Mutation of this residue to an Ala increased the autoprocessing activity of *Tb*MCA2. All the *Sc*MC prodomains except *Sc*MC3 contain several Tyr residues, but sequence variation makes alignment of this region unreliable (SI Fig. 2).

Several regions have been identified as sites of proteolysis in metacaspases. The first is between the N-terminal domain and the p20 region and the second is between the p20 and p10 regions. In all five *Sc*MCs a sequence between the N-terminal domain and the p20 region that is enriched in Lys and Arg residues aligns well with a similar sequence that is cleaved in *At*MC1 [19] (Fig. 2). The Lys that is cleaved in *Tb*MCA2 [11] is within 20aa of these residues. The potential proteolysis site is also well conserved in multicellular fungal metacaspases (SI Fig. 2) [20]. In the linker between the p20 and p10 regions, cleavage sites have been identified in the *A. thaliana* metacaspases (an Arg) and in *S. cerevisiae* MCA1 (a Lys) [19]. The Lys in MCA1 aligns with a Lys in *Sc*MC1 (Fig. 2). Sequences of multicellular fungi (including *S. commune)* typically have both Lys and/or Arg in abundance in this region. Based on sequence, a site for proteolysis between the p20 and p10 regions is not well-conserved. This is consistent with the fact that proteolytic processing of metacaspases does not appear to be required for activity [5,11].

3.2. Cloning and expression

The cloning template cDNA was *S. commune* strain T26 leading to some differences when compared with the sequences from *S. commune* strain H48 in the NCBI database. In *Sc*MC2 the Ser53 codon is AGC instead of TCC, and in *Sc*MC5 there is a 6 nucleotide in-frame insertion after position 501 leading to an additional 2 aa (His, Gly). A larger difference is present in *Sc*MC3 due to a splice prediction error in the database at nucleotide 642 that leads to a 74 base insertion, a frame shift, and the use of a different stop

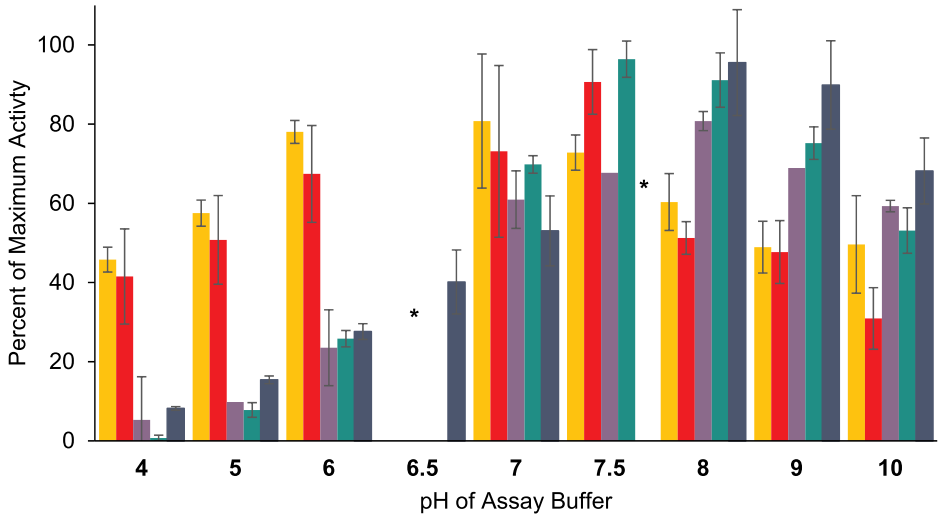

Fig. 3. Activity of all five metacaspases at varying assay buffer pH. The activity of each protein at its optimal calcium concentration with Z-GGR-AMC substrate [*Sc*MC1(yellow), *Sc*MC2(red), *Sc*MC3 (purple), *Sc*MC4(green), *Sc*MC5(blue)]. Data are plotted as a percentage of the highest value. Three trials were performed for each protein at each pH. Error bars represent standard deviations. (*Denotes missing data at pH 6.5 for *Sc*MC1-4 and at pH 7.5 for *Sc*MC5.)

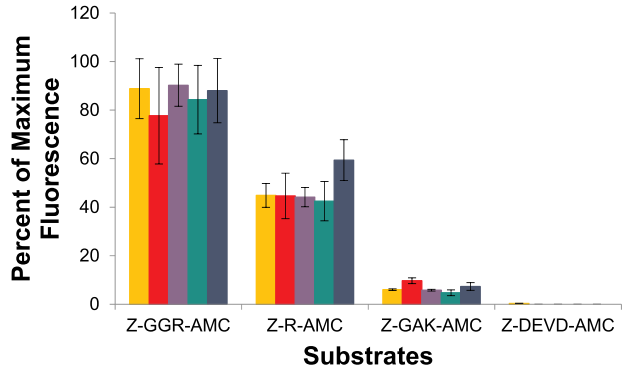

Fig. 4. Activity of all five metacaspases with peptide substrates. The activity of each protein at pH 7.5 and optimal calcium concentration (50 mM Ca^{2+} for *Sc*MC1 and 2; 5 mM Ca^{2+} for *Sc*MC3-5) is shown above the name of the substrate [*Sc*MC1(yellow), *Sc*MC2(red), *Sc*MC3(purple), *Sc*MC4(green), *Sc*MC5(blue)]. Data are plotted as a percentage of the highest value. Three trials were performed for each protein with each substrate. Error bars represent standard deviations.

codon that extends the protein sequence at the C-terminus.

*Sc*MC3 is the only protein that can be expressed in traditional HIS-tag fusion vectors such as pQE (Qiagen) and pET (Novagen). While *Sc*MC3 protein is produced in these systems, it is found in insoluble aggregates. *Sc*MC1,2,4, and 5 only express well when the small ubiquitin-related modifier (SUMO) sequence is fused via a linker to the N-terminus of each protein. When linked to the SUMO sequence, *Sc*MC1-5 are both well-expressed and soluble. N-terminal attachment of SUMO promotes correct folding in a variety of proteins expressed in *E. coli* without interfering with the catalytic activity of the enzymes. SUMO may promote of folding either by slowing the aggregation process or by providing a nucleation site for proper folding [21]. This is the first report of the use of SUMO for the expression of metacaspases.

Each metacaspase was cloned both with and without (Δpro) the putative prodomain. The location of the prodomain deletion was determined by comparing the *Sc*MC sequences with the cleavage site in *At*MC1 to locate the start of the p20-like catalytic region (see Fig. 1 and SI Fig. 2 for locations of the sequence start in Δpro constructs). This site was examined in the three-dimensional structures of *Tb*MCA2 and Yca1 to avoid cleavage that was likely to be important for tertiary structure. The C-terminus of the deletion is the residue that aligns with the N-terminus of strand β1, so the Δpro constructs begin with the amino acid that aligns with the second residue of this β strand [11]. This residue aligns with the cleavage site between the prodomain and the p20-like region in plant metacaspases [19]. Since the prodomain for *Sc*MC3 is less than 10 residues in length, it was only cloned and expressed as the full length protein. For *Sc*MC1, 2, 4, and 5 both forms of the protein had similar enzymatic activity against peptide substrates, but the presence of the prodomain produced more complex banding patterns on SDS gels suggesting that more than one form of the metacaspase may be involved in catalysis. Therefore, it was not possible to know what fragments of the constructs with the prodomains were responsible for cleavage during activity assays, or what regulatory regions these fragments contained. The data presented here is focused on the forms without the prodomain (Δpro) to allow for a more accurate characterization of the the active region of the *S. commune* metacaspase proteins.

3.3. Metacaspase activity

All five *Sc*MCΔpro proteins have the highest enzymatic activity between pH 7–8 (Fig. 3), consistent with other metacaspases [7,12,19,22,23]. The active site His will be at least partially deprotonated in this pH range, allowing it to act as a base to increase the nucleophilicity of the active site Cys in the reaction mechanism. Mutation of both active site residues (His 264 to Gln and Cys 320 to Ala) in *Sc*MC1 produced an enzyme with ~1% of the wild-type activity demonstrating the importance of these residues for catalysis (SI Table 4).

All five *S. commune* metacaspases have similar substrate specificity (Fig. 4). The Z-GGR-AMC substrate is cleaved most rapidly, indicating preference for Arg at the cleavage site (P1) and smaller amino acids in the P2 and P3 sites. For *Sc*MC1-5Δpro, the Z-R-AMC substrate had less than 60% of the activity compared to Z-GGR-AMC, indicating that the presence of residues in the P2 and P3 sites increases activity. A peptide with Lys at the P1 site, Z-GAK-AMC, was processed at a lower rate than either Arg-containing peptide, and showed only 10% of the activity produced in the presence of Z-GGR-AMC. Like many other metacaspases, the *Sc*MC are more active against small peptides with arginine at the cleavage site than with lysine at the cleavage site [22,24]. The caspase substrate Z-DEVD-AMC was not processed by any of the metacaspases tested (Fig. 4). Caspases are aspartic acid specific, while metacaspases cleave after arginine and lysine.

All five metacaspases were more active in the presence of millimolar levels of calcium ions. Optimal Ca^{2+} concentrations for *Sc*MC1Δpro and *Sc*MC2Δpro were high (50 mM) (Fig. 5) and the enzymes were most active over similar ranges of Ca^{2+} concentrations. The activity of *Sc*MC3,

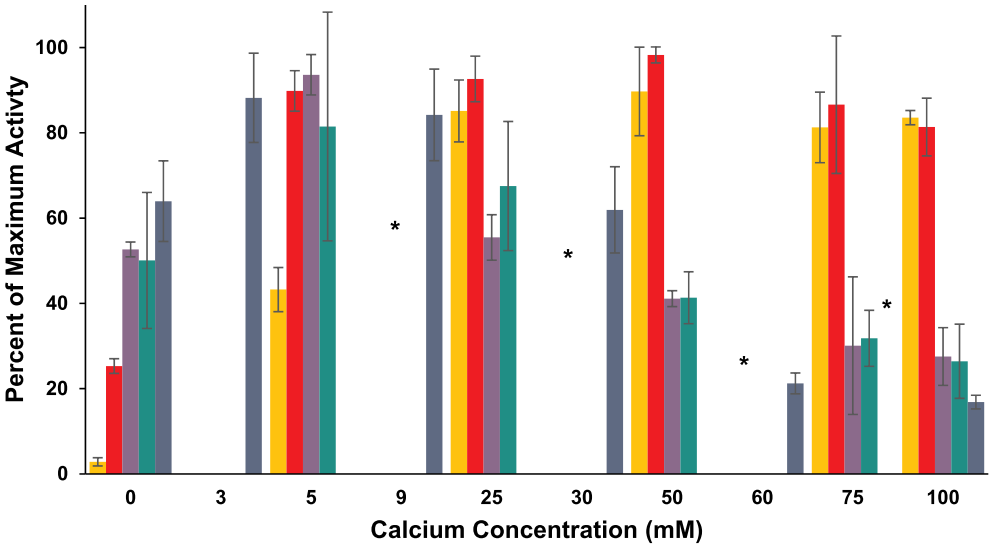

Fig. 5. Activity of all five metacaspases at varying calcium concentrations. The activity of each protein was determined at pH 7.5 with Z-GGR-AMC substrate [*Sc*MC1 (yellow), *Sc*MC2(red), *Sc*MC3(purple), *Sc*MC4(green), *Sc*MC5(blue)]. Data are plotted as a percentage of the highest value. Three trials were performed for each protein with at each calcium concentration. Error bars represent standard deviations. (*Denotes missing data at 9mM, 30 mM, and 60 mM calcium for *Sc*MC1-4 and at 25, 50 mM, and 75 mM calcium for *Sc*MC5.)

*Sc*MC4Δpro and *Sc*MC5Δpro is optimal around 5 mM calcium and noticeably decreases above 30 mM calcium. Only *Sc*MC1Δpro is completely inactive in the absence of calcium, while *Sc*MC2Δpro, *Sc*MC3, *Sc*MC4Δpro and *Sc*MC5Δpro retain partial activity without calcium (Fig. 5). The optimal calcium concentrations obtained for all five *Sc*MC proteins are similar to results of other characterized metacaspases [10,19,25].

During purification *Sc*MC1Δpro remains intact and produces a single band on an SDS gel (SI Fig. 1) and Western Blot (data not shown). This is consistent with the fact that *Sc*MC1Δpro absolutely requires calcium for activity. The concentration of calcium present in the purification buffers is very low and this prevents *Sc*MC1 from undergoing any autoprocessing. The other four *S. commune* metacaspases (*Sc*MC2-5Δpro) produce more complex banding patterns on SDS gels (SI Fig. 1) and Western blots (data not shown) due to their autoproteolytic activity even in the absence of calcium.

Studies on the enzymes with the prodomains (+pro) were complicated by moderate expression levels and proteins with very low specific activities. For example, *Sc*MC1 + pro had only ~5% the specific activity of *Sc*MC1Δpro (SI Table 4). Metacaspases typically have relatively low catalytic efficiencies and undergo autoproteolysis during concentration and storage. As a result, reliable studies of wild-type full-length protein are difficult due to the presence of multiple proteolysis products. Enough *Sc*MC1 + pro was purified to perform activity assays. The pH optimum and substrate specificity were the same for *Sc*MC1Δpro and *Sc*MC1 + pro (Fig. 6). However, the activity of the enzyme including the

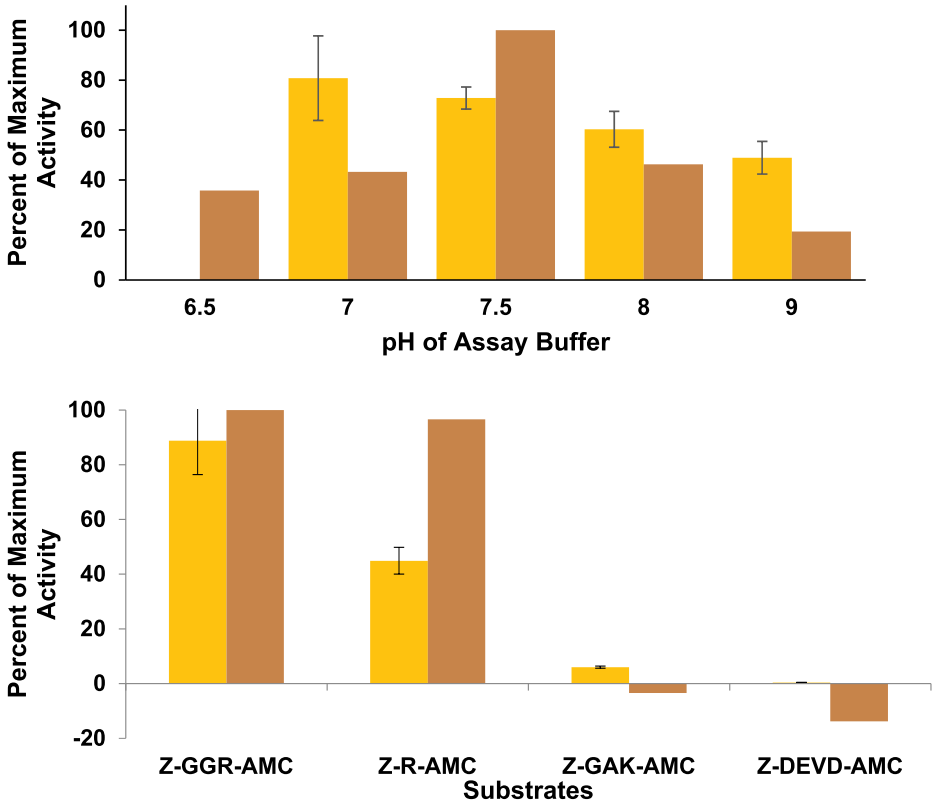

Fig. 6. Comparison of the activity of *Sc*MC1 at varying pH and [calcium] with the putative prodomain (+pro, brown) and without (Δpro, yellow) the putative prodomain. Assays were done at pH 7.5 and 5 mM calcium with Z-GGR-AMC substrate. Data are plotted as a percentage of the highest value. Three trials were performed for *Sc*MC1Δpro and a single trial for *Sc*MC1 + pro. Error bars represent standard deviations.

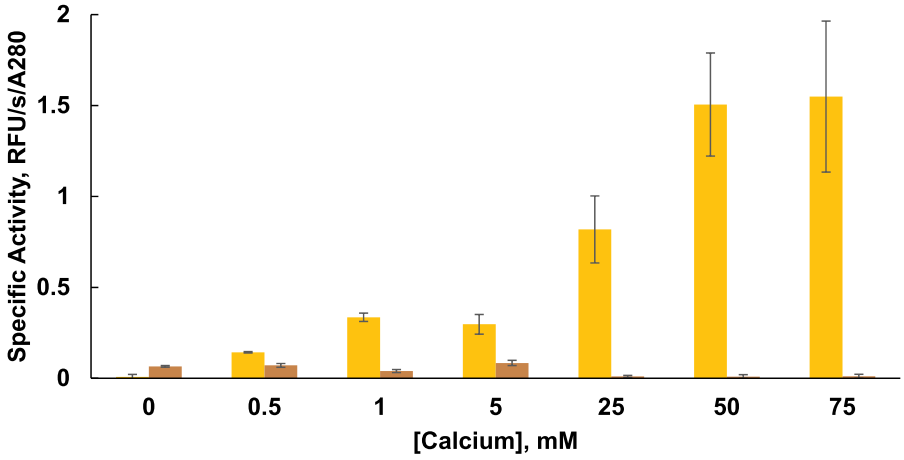

Fig. 7. Comparison of the activity against peptide substrates of *Sc*MC1 with the putative prodomain (+pro, brown) and without (Δpro, yellow) the putative prodomain. Assays were done at pH 7.5 with Z-GGR-AMC substrate. Enzyme activity data in relative fluorescence units/second are corrected for the amount of protein by dividing by absorbance at 280 nm. Three trials were performed for each protein. Error bars represent standard deviations.

prodomain is much lower at all calcium concentrations, and adding calcium does not result in a significant increase in activity (Fig. 7). The enzyme without the prodomain is strongly activated by increasing calcium concentrations.

While the active sites seem to function similarly in different forms of the enzyme, enzyme activity is regulated by calcium levels and autoproteolysis. This is consistent with recent work in plants showing that metacaspases can be activated *in vivo* both by autocatalytic cleavage of the metacaspase and by increases in calcium levels [26].

4. Conclusions

Five Type I metacaspases in the fungus *Schizophyllum commune* have been identified and characterized. The multicellular basidomycete *S. commune* is a member of the group of mushroom-forming fungi; has roles in human health, agriculture, and biotechnology; and is the only member of this group of organisms that can be cultured on defined media. This makes it an attractive model for metacaspase function *in vivio* in basidiomycetes. Analysis of the sequences of the *Sc*MC proteins reveals significant similarities between the yeast, plant and *T. brucei* metacaspases at residues involved in reactivity and substrate specificity that are the most well-characterized in the literature. Despite the sequence similarity among the five *S. commune* metacaspases, the difference in response to calcium by *Sc*MC1 when compared to the other *Sc*MC proteins suggests that each enzyme may play a specific physiological role. *Sc*MC1 could play a critical role in cellular pathways where calcium dependence helps regulate enzymatic activity. In yeast, metacaspases have been shown to cleave the DNA-damage inducible protein 1 (Ddi1), and it is known that Ddi1 cleavage is regulated by changes in calcium concentrations [27]. Ca^{2+} signaling is a frequently observed response to cell death inducing compounds in fungi [2]. Intracellularly, free calcium concentration is typically in the nanomolar range and total calcium (free + bound) is in the low millimolar range [28], so only in the presence of a dramatic increase in calcium concentration would a response from *Sc*MC1 be physiologically relevant.

Acknowledgements

We would like to thank Stephanie Scharbach for her contributions to cloning and expression of *Sc*MC2, J. Stephen Horton for providing the *S. commune* cDNA library and advice on working with the *S. commune* genome sequence, and Michelle Richter for helpful comments on the manuscript. We thank the Union College Faculty Research fund and Student Research Grants for funding.

Appendix A. Supplementary data

Supplementary data to this article can be found online at https://doi.org/10.1016/j.bbrep.2019.100706.

Transparency document

Transparency document related to this article can be found online at https://doi.org/10.1016/j.bbrep.2019.100706.

References

[1] A.G. Uren, K. O'Rourke, L. Aravind, M.T. Pisabarro, S. Seshagiri, E.V. Koonin, V.M. Dixit, Identification of paracaspases and metacaspases: two ancient families of caspase-like proteins, one of which plays a key role in MALT lymphoma, Mol. Cell 6 (2000) 961–967, https://doi.org/10.1016/S1097-2765(05)00086-9.
[2] A.P. Gonçalves, J. Heller, A. Daskalov, A. Videira, N.L. Glass, Regulated forms of cell death in fungi, Front. Microbiol. 8 (2017) 1837, https://doi.org/10.1038/msb.2011.75.
[3] Y. Fuchs, H. Steller, Programmed cell death in animal development and disease, Cell 147 (2011) 742–758, https://doi.org/10.1016/j.cell.2011.10.033.
[4] K. McLuskey, J.C. Mottram, Comparative structural analysis of the caspase family with other clan CD cysteine peptidases, Biochem. J. 466 (2015) 219–232, https://doi.org/10.1042/BJ20141324.
[5] L. Tsiatsiani, F. Van Breusegem, P. Gallois, A. Zavialov, E. Lam, P.V. Bozhkov, Metacaspases, Cell Death Differ. 18 (2011) 1279–1288, https://doi.org/10.1038/cdd.2011.66.
[6] A. Sharon, A. Finkelstein, N. Shlezinger, I. Hatam, Fungal apoptosis: function, genes and gene function, FEMS Microbiol. Rev. 33 (2009) 833–854, https://doi.org/10.1111/j.1574-6976.2009.00180.x.
[7] P.V. Bozhkov, M.F. Suarez, L.H. Filonova, G. Daniel, A.A. Zamyatnin Jr., S. Rodriguez-Nieto, B. Zhivotovsky, A. Smertenko, Cysteine protease mcII-Pa executes programmed cell death during plant embryogenesis, Proc. Natl. Acad. Sci. U.S.A. 102 (2005) 14463–14468, https://doi.org/10.1073/pnas.0506948102.
[8] N.D. Rawlings, A.J. Barrett, P.D. Thomas, X. Huang, A. Bateman, R.D. Finn, The MEROPS database of proteolytic enzymes, their substrates and inhibitors in 2017 and a comparison with peptidases in the PANTHER database, Nucleic Acids Res. 46 (2018) 624–632, https://doi.org/10.1093/nar/gkx1134.
[9] E.A. Minina, N.S. Coll, H. Tuominen, P.V. Bozhkov, Metacaspases versus caspases in development and cell fate regulation, Cell Death Differ. 24 (2017) 1314–1325, https://doi.org/10.1038/cdd.2017.18.
[10] M. Klemenčič, C. Funk, Type III metacaspases: calcium-dependent activity proposes new function for the p10 domain, New Phytol. 218 (2017) 1179–1191, https://doi.org/10.1111/nph.14660.
[11] K. McLuskey, J. Rudolf, W.R. Proto, N.W. Isaacs, G.H. Coombs, C.X. Moss, J.C. Mottram, Crystal structure of a *Trypanosoma brucei* metacaspase, Proc. Natl. Acad. Sci. 109 (2012) 7469–7474, https://doi.org/10.1073/pnas.1200885109.
[12] A.H.H. Wong, C. Yan, Y. Shi, Crystal structure of the yeast metacaspase Yca1, J. Biol. Chem. 287 (2012) 29251–29259, https://doi.org/10.1074/jbc.M112.381806.
[13] C. Pop, G.S. Salvesen, Human caspases: activation, specificity, and regulation, J. Biol. Chem. 284 (2009) 21777–21781, https://doi.org/10.1074/jbc.R800084200.
[14] J.M. Gilio, M.F. Marcondes, D. Ferrari, M.A. Juliano, L. Juliano, V. Oliveira, M.F.M. Machado, Processing of metacaspase 2 from *Trypanosoma brucei* (TbMCA2) broadens its substrate specificity, Biochim. Biophys. Acta Protein Proteonomics 1865 (2017) 388–394, https://doi.org/10.1038/cdd.2011.66.
[15] C.X. Moss, G.D. Westrop, L. Juliano, G.H. Coombs, J.C. Mottram, Metacaspase 2 of *Trypanosoma brucei* is a calcium-dependent cysteine peptidase active without

processing, FEBS Lett. 581 (2007) 5635–5639, https://doi.org/10.1016/j.febslet.2007.11.009.
[16] R.A. Ohm, J.F. De Jong, L.G. Lugones, A. Aerts, E. Kothe, J.E. Stajich, R.P. De Vries, E. Record, A. Levasseur, S.E. Baker, Genome sequence of the model mushroom *Schizophyllum commune*, Nat. Biotechnol. 28 (2010) 957–963, https://doi.org/10.1038/nbt.1643.
[17] F. Sievers, A. Wilm, D. Dineen, T.J. Gibson, K. Karplus, W. Li, R. Lopez, H. McWilliam, M. Remmert, J. Soding, J.D. Thompson, D.G. Higgins, Fast, scalable generation of high-quality protein multiple sequence alignments using Clustal Omega, Mol. Syst. Biol. 18 (2011) 1279–1288, https://doi.org/10.1038/msb.2011.75 ([doi]).
[18] G. Yachdav, E. Kloppmann, L. Kajan, M. Hecht, T. Goldberg, T. Hamp, P. Hönigschmid, A. Schafferhans, M. Roos, M. Bernhofer, PredictProtein—an open resource for online prediction of protein structural and functional features, Nucleic Acids Res. 42 (2014) W337–W343, https://doi.org/10.1093/nar/gku366.
[19] N. Watanabe, E. Lam, Calcium-dependent activation and autolysis of *Arabidopsis* metacaspase 2d, J. Biol. Chem. 286 (2011) 10027–10040, https://doi.org/10.1074/jbc.M110.194340.
[20] M. Ojha, A. Cattaneo, S. Hugh, J. Pawlowski, J.A. Cox, Structure, expression and function of *allomyces arbuscula* CDP II (metacaspase) gene, Gene 457 (2010) 25–34, https://doi.org/10.1016/j.gene.2010.02.014.
[21] J.G. Marblestone, S.C. Edavettal, Y. Lim, P. Lim, X.U.N. Zuo, T.R. Butt, Comparison of SUMO fusion technology with traditional gene fusion systems: enhanced expression and solubility with SUMO, Protein Sci. 15 (2006) 182–189, https://doi.org/10.1110/ps.051812706.
[22] N. Lee, S. Gannavaram, A. Selvapandiyan, A. Debrabant, Characterization of metacaspases with trypsin-like activity and their putative role in programmed cell death in the protozoan parasite *Leishmania*, Eukaryot. Cell 6 (2007) 1745–1757, https://doi.org/10.1128/EC.00123-07.
[23] M.F.M. Machado, M.F. Marcondes, M.A. Juliano, K. McLuskey, J.C. Mottram, C.X. Moss, L. Juliano, V. Oliveira, Substrate specificity and the effect of calcium on *Trypanosoma brucei* metacaspase 2, FEBS J. 280 (2013) 2608–2621.
[24] N. Watanabe, E. Lam, Two arabidopsis metacaspases AtMCP1b and AtMCP2b are arginine/lysine-specific cysteine proteases and activate apoptosis-like cell death in yeast, J. Biol. Chem. 280 (2005) 14691–14699, https://doi.org/10.1074/jbc.M413527200.
[25] E. Piszczek, M. Dudkiewicz, M. Mielecki, Biochemical and bioinformatic characterization of type II metacaspase protein (TaeMCAII) from wheat, Plant Mol. Biol. Report. 30 (2012) 1338–1347, https://doi.org/10.1007/s11105-012-0450-6.
[26] T. Hander, Á.D. Fernández-Fernández, R.P. Kumpf, P. Willems, H. Schatowitz, D. Rombaut, A. Staes, J. Nolf, R. Pottie, P. Yao, A. Gonçalves, B. Pavie, T. Boller, K. Gevaert, F. Van Breusegem, S. Bartels, S. Stael, Damage on plants activates Ca 2+ -dependent metacaspases for release of immunomodulatory peptides, Science (2019) 363, https://doi.org/10.1126/science.aar7486 80-.
[27] L.A. Bouvier, G.T. Niemirowicz, E. Salas-Sarduy, J.J. Cazzulo, V.E. Alvarez, DNA-damage inducible protein 1 is a conserved metacaspase substrate that is cleaved and further destabilized in yeast under specific metabolic conditions, FEBS J. 285 (2018) 1097–1110, https://doi.org/10.1111/febs.14390.
[28] R. Milo, P. Jorgensen, U. Moran, G. Weber, M. Springer, BioNumbers—the database of key numbers in molecular and cell biology, Nucleic Acids Res. 38 (2010) D750–D753, https://doi.org/10.1093/nar/gkp889.